Journal of Nuclear Materials 390–391 (2009) 733–739

Contents lists available at ScienceDirect

Journal of Nuclear Materials

journal homepage: www.elsevier.com/locate/jnucmat

Active control of edge localized modes with a low *n* perturbation fields in the JET tokamak

Y. Liang [b,*], S. Jachmich [c], H.R. Koslowski [b], E. Nardon [d], A. Alfier [e], Y. Baranov [d], E. De La Luna [f], P. de Vries [d], T. Eich [g], H.G. Esser [b], D. Harting [b], V. Kiptily [d], A. Kreter [b], S. Gerasimov [d], M.P. Gryaznevich [d], D. Howell [d], G. Sergienko [b], JET–EFDA contributors [a,1]

[a] *JET–EFDA, Culham Science Centre, OX14 3DB Abingdon, UK*
[b] *Association EURATOM–FZJ, Forschungszentrum Jülich GmbH, Institute of Energy Research IEF-4: Plasma Physics, Partner in the Trilateral Euregio Cluster, 52425 Jülich, Germany*
[c] *Association EURATOM–Belgian State, Koninklijke Militaire School – Ecole Royale Militaire, B-1000 Brussels, Belgium*
[d] *EURATOM–UKAEA Fusion Association, Culham Science Centre, OX14 3DB Abingdon, OXON, UK*
[e] *Associazione EURATOM–ENEA sulla Fusione, Consorzio RFX Padova, Italy*
[f] *Asociación EURATOM–CIEMAT, Avenida Complutense 22, E-28040 Madrid, Spain*
[g] *Association EURATOM–Max-Planck-Institut für Plasmaphysik, D-85748 Garching, Germany*

ARTICLE INFO

PACS:
28.52.−s
52.35.Py
52.55.Fa
52.55.Rk

ABSTRACT

Active control of edge localized modes (ELMs) by using static external magnetic perturbation fields with low toroidal mode number, *n*, has been demonstrated for both, ITER baseline ($q_{95} \sim 3$) and high beta advanced tokamak scenarios at the JET tokamak. During the application of the low *n* field the ELM frequency increased by a factor up to ~4–5. Reduction in carbon erosion and ELM peak heat fluxes on the divertor target by roughly the same factor as the increase of the ELM frequency has been observed. The frequency of the mitigated ELMs using a low *n* field is found to increase proportional to the total input heating power. Compensation of the density pump-out effect observed when the external low *n* field is applied has been achieved by gas fueling in low triangularity plasmas.

1. Introduction

The standard tokamak H-mode, which is foreseen as the ITER baseline operating scenario [1], is characterised by a steep plasma pressure gradient and associated increased current density at the edge transport barrier which exceeds a threshold value to drive magnetohydrodynamic (MHD) instabilities referred to as edge localized modes (ELMs) [2,3]. The so-called type-I ELMs lead to a periodic expulsion of a considerable fraction of the stored energy content onto the plasma facing components. Although ELMs may be beneficial in controlling the particle inventory and removing fusion products, the associated energy losses might cause severe problems regarding the life time expectations of plasma facing wall components. Melting or high erosion rates might occur under certain conditions as derived from extrapolations based on present knowledge [4]. Therefore, reliable methods for the control of type-I ELM power losses are required for operation of a future fusion machine, e.g. ITER [1].

Previous experiments on DIII-D have shown that the application of resonant magnetic perturbation fields (RMP) is a promising technique for the complete suppression of ELMs with an $n = 3$ field induced by a set of in-vessel coils [5,6]. On JET, active control of the transient heat loads due to large type-I ELMs has been achieved with low-*n* ($n = 1$ and $n = 2$) fields induced by the set of error field correction coils (EFCCs) [7] mounted outside of the vacuum vessel [8,9].

During the application of the $n = 1$ field the ELM frequency increased by a factor of 4–5 for a duration of 10 times the energy confinement time. The energy loss per ELM normalized to the total stored energy, $\Delta W/W$, decreased from 7% to values below the resolution limit of the diamagnetic measurement (~2%). The density pump-out effect [10], the reduction in ELM amplitude, the simultaneous increase in ELM frequency and braking of the plasma toroidal rotation [11] were observed independent on the toroidal phase (i.e. the direction in the tokamak midplane) of the $n = 1$ field [8]. Recently, the operational domain for active control of type-I ELMs with an $n = 1$ field has been developed toward more ITER relevant regimes with high plasma triangularity ($\delta^{upper} \sim 0.45$ and $\delta^{lower} \sim 0.4$), high normalized beta (up to 3.0), plasma current up to 2.0 MA and q_{95} varied between 3.0 and 4.8. In those experiments, no additional gas fueling was applied. The Greenwald

* Corresponding author.
E-mail address: y.liang@fz-juelich.de (Y. Liang).

[1] See the Appendix of M.L. Watkins et al., Fusion Energy 2006 (Proceedings of 21st International Conference, Chengdu) IAEA, 2006.

0022-3115/$ - see front matter © 2009 Published by Elsevier B.V.
doi:10.1016/j.jnucmat.2009.01.199

fraction, f_{GW}, for those target plasmas is in the range of 0.65–0.8. The minimum $n = 1$ perturbation field amplitude above which the ELMs were mitigated increased when q_{95} was lowered, but always remained below the $n = 1$ locked mode threshold. The results of ELM mitigation experiments with $n = 2$ magnetic perturbations on JET showed that the frequency of ELMs could be increased from 10 Hz to 35 Hz [9]. A wide operational window of q_{95} from 4.5 to 3.1 has also been found with $n = 2$ field without observation of any locked mode even at the maximum value of EFCC coil current delivered from the present power supply system. Transport analysis using the TRANSP code [12] shows no or a modest reduction of the thermal energy confinement time, τ_{therm}, mainly attributed to the density pump-out, but when τ_{therm} was normalized to the IPB98(y,2) scaling [1] the confinement showed almost no reduction. However, for a possible application of this method for ELM control in a future reactor, the important question of how the density pump-out could be compensated and the plasma confinement maintained, has to be resolved.

In this paper, the application of active ELM control with a low n field in the ITER baseline ($q_{95} \sim 3$) and high beta advanced tokamak steady state scenarios is discussed. The influence of mitigated ELMs on carbon erosion and the heat flux onto the divertor and limiter tiles are described. The heating power dependence of the ELM frequency of mitigated ELMs by an $n = 1$ field is studied. Furthermore, the first experimental results of pump-out compensation with gas fueling in a low triangularity plasma are presented.

2. Application of $n = 1$ fields for ELM mitigation in AT scenario

Advanced tokamak steady state (AT) scenarios operate at a normalized beta close to or above the no-wall beta limit. In this scenario ELM mitigation is needed to keep ELM amplitudes small which otherwise may erode the internal transport barrier and reduce the confinement [13,14].

Fig. 1 shows an example where the $n = 1$ fields have been applied for ELM control in AT scenarios at high β_N ($B_t = 1.8$ T, $I_p = 1.2$ MA, $q_{95} = 4.5$). Real-time beta control has been applied to maintain a prescribed $\beta_N \sim 2.5$ (approximate no-wall beta limit $4 \times \ell_i$) by controlling the NBI input power. The ELMs in the target plasma have the standard Type I characteristics with an edge transport barrier that provides a normalized thermal confinement of $H_{IPB98(y,2)} \sim 1$. When the current in the EFCCs I_{EFCC} is ramped up the D_α spikes show a strong decrease in magnitude and the ELM frequency increases. The effective radial resonance magnetic perturbations, $|b_r^{n=1}/B_t|$, measured at the low field side of the in-vessel wall by a set of saddle coils for $I_{EFCC} = 24$ kAt is $\sim 3.6 \times 10^{-3}$. Although the density decreases due to the pump-out effect, transport analysis using the TRANSP code shows that the thermal energy stays almost constant. Another indication for the constant energy content is given by the unchanged heating power request from the real-time beta control. This is due to the fact that both, ion and electron temperatures, T_i and T_e, increase, similar to the previous observation in standard ELMy H-modes [8].

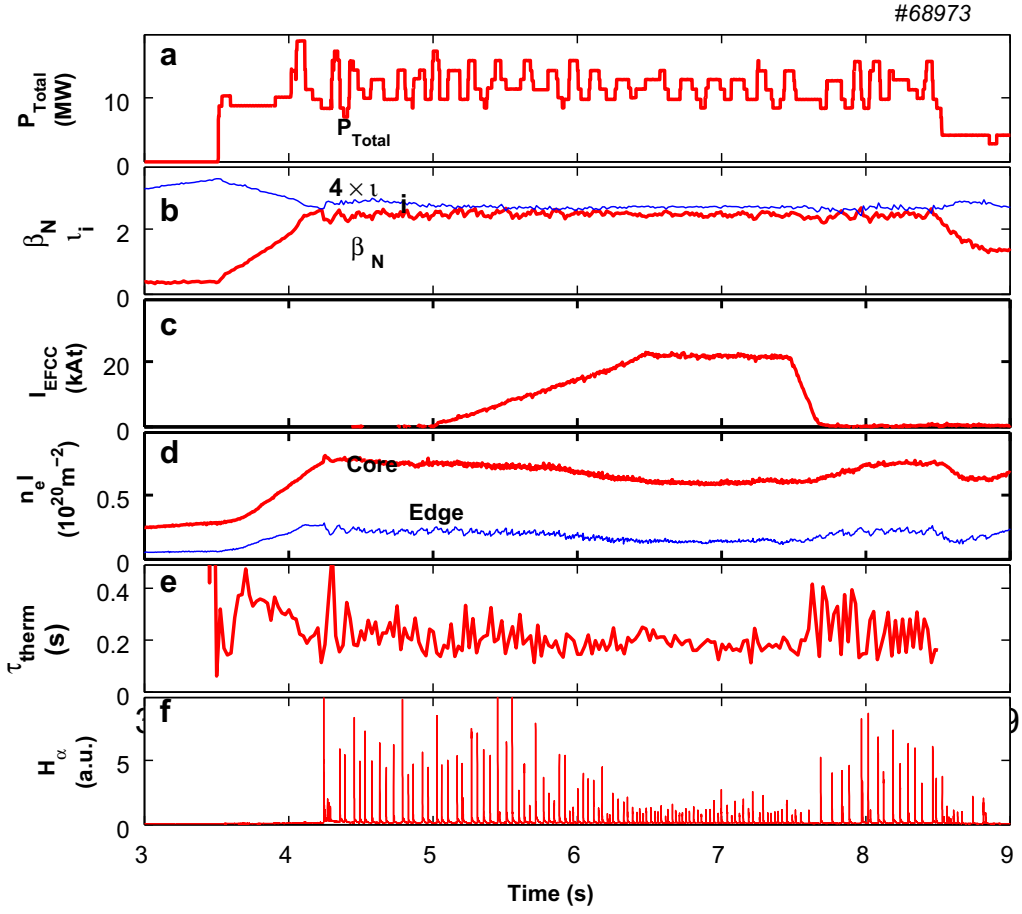

Fig. 1. Time evolution of (a) the total input power, P_{Total}, (b) normalized beta, β_N and internal inductance, l_i, (c) I_{EFCC}, (d) line integrated electron densities, $n_e l$, measured with an interferometer along two lines of sight, one close to the magnetic axis (upper trace) and the other near the pedestal top (lower trace), (e) thermal energy confinement time, τ_{therm} and (f) D_α signal measured at the outer divertor for a high beta discharge.

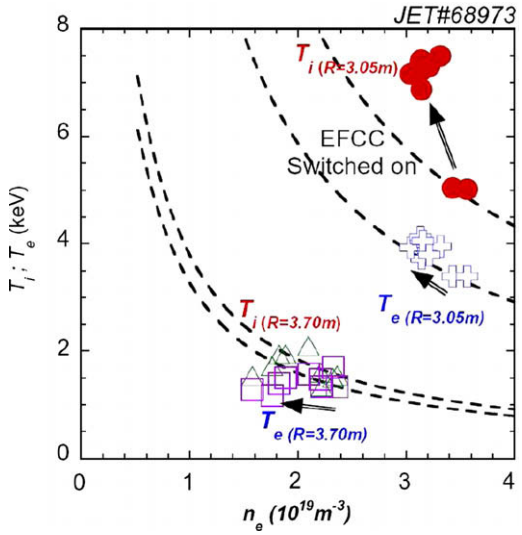

Fig. 2. Evolution of T_i and T_e as a function of electron density, n_e, for the same high beta discharge as shown in Fig. 1. The arrows indicate the change when the EFCC is switched on.

Fig. 2 shows that the influence of the $n = 1$ field on T_i, T_e and n_e in the plasma core ($R = 3.05$ m) and near the edge pedestal ($R = 3.70$ m). The dashed curves indicate a constant plasma thermal pressure. Due to application of the $n = 1$ field, the edge plasma pressure dropped by ~20% caused by the reduction of edge n_e while both, edge T_i and T_e stay almost constant. However, the ion pressure increase in the plasma core due to the rise of T_i form ~ 5 to ~7.5 keV over compensated the drop of n_e, while the core electron pressure remains constant.

Active control of type-I ELMs with the $n = 1$ field was successfully applied in similar discharges with β_N up to 2.9, but further technical development will be required to increase the pulse duration capability of the EFCC system at the required large coil currents. It is also important to note that in these experiments no locked modes were seeded by the perturbation field. It is quite likely that the strong beam heating keeps the toroidal plasma rotation high enough to prevent the field from penetrating [15,16].

3. Heat load and carbon erosion of mitigated ELMs

The heat loading and carbon erosion of the divertor target due to mitigated ELMs by an $n = 1$ field has been studied in a series of high triangularity discharges ($\delta = 0.45$) [17]. During the flat top of a the type-I ELMy H-mode phase ($I_p = 1.8$ MA, $B_t = 2.16$ T, $q_{95} = 4.4$, $P_{NBI} = 9.5$ MW, $n_e l = 1.3 \times 10^{20}$ m^{-2}, $f_{GW} = 0.7$) the error field correction coils at a current of 32 kAt have been applied. The ELM frequency increases from 30 Hz up to 90 Hz, while the loss of stored energy per ELM, ΔW decreases from ~ 130 kJ to less than ~ 50 kJ which lie within the noise level (2%) of the diamagnetic measurement.

Fig. 3 shows profiles of (a) particle flux, (b) electron temperature and (c) heat flux measured near the outer strike point for the cases with and without the application of the $n = 1$ field. Here, the heat fluxes are measured by Langmuir Probes (LP) embedded in the divertor tiles. When the magnetic perturbation field is applied, a reduction in the ELM peak heat fluxes on the divertor target by roughly the same factor as the increase of the ELM frequency has been observed. The loss of core and edge density (density pump-out effect) during the application of the $n = 1$ field is not seen as an increased particle flux at the divertor in neither the inter-ELM phase nor at the ELM peak as shown in Fig. 3. The reduction in heat

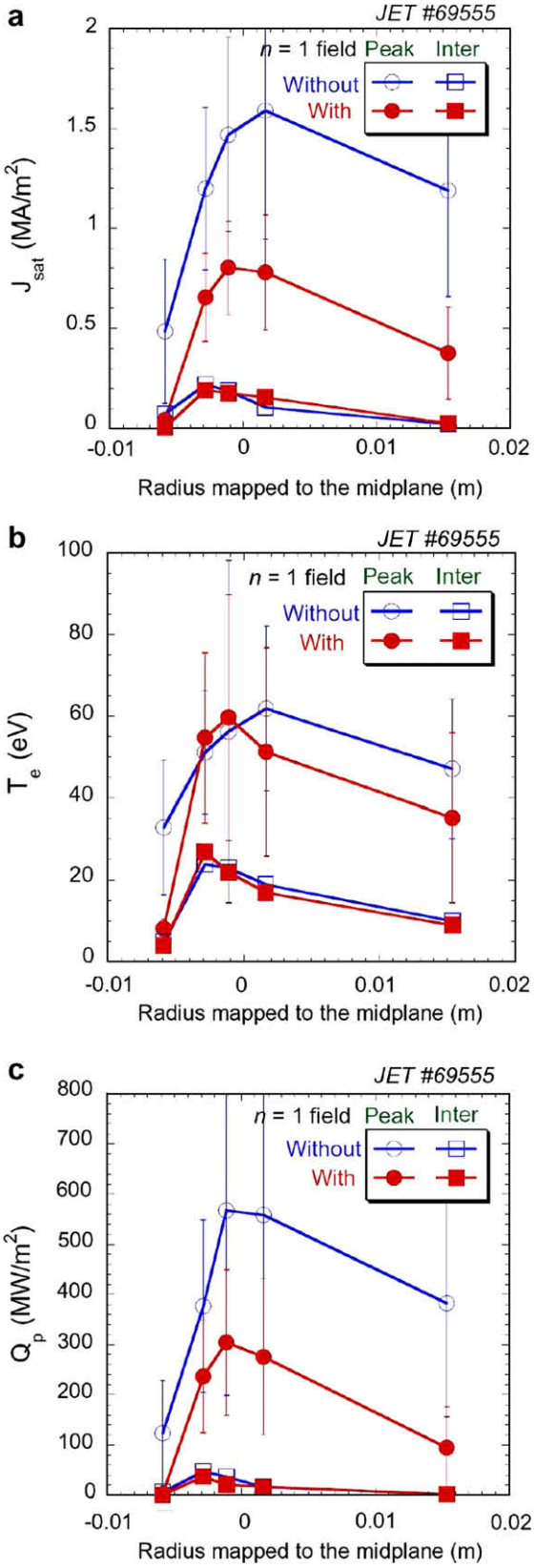

Fig. 3. Profiles of (a) particle flux, (b)temperature and (c) heat flux at the outer divertor strike point.

flux is mainly due to the drop of particle flux rather than the change of the electron temperature. It is important to note that

the electron temperature remains unaffected (Fig. 3), also in the inter-ELM phase. No clear changes in heat flux during the inter-ELM phase has been observed, which is consistent with the observation of only small changes of the global plasma confinement. A similar observation has been made by a fast IR camera viewing the divertor targets. The measurement of the LP array on JET is located in one toroidal cross section. However, the reduction of the heat flux on the dirvertor plates with application of the external field has been observed in discharges with different EFCC phasings. These observations do not depend on the toroidal phase of the $n = 1$ perturbation field. Furthermore, the particle flux measured with the outer wall guard limiter probes shows that the interaction of the ELMs with the outer wall is also significantly reduced.

In addition, the results from the quartz microbalance (QMB) [18] measuring the amount of carbon deposited in the inner divertor louvre indicates clearly less erosion of carbon from the divertor in phases with mitigated ELMs. In type-I ELMy H-mode plasmas, net-deposition of carbon on the QMB with a growth rate of ~ 0.6 nm/s was observed. However, when the large ELMs were mitigated by $n = 1$ field, net-erosion of carbon from the QMB (~ 0.25 nm/s) was observed, which is mainly due to a significant deuterium flux even when the carbon flux shows a strong reduction.

4. Application of $n = 1$ fields for ELM mitigation in the ITER baseline scenario

Active ELM control has been investigated in the ITER baseline scenario operated at $q_{95} \sim 3$. For the $n = 1$ field, it is more critical since the previous experimental results show that the operational window for the ELM control becomes narrow because the minimum value of perturbation field to effect ELMs increases and the locked mode threshold decreases at lower q_{95}.

In this experiment, the target plasma was heated by NBI with a power of 14 MW. q_{95} is ~ 3.2 at I_p of 2 MA and B_t of 1.85 T. Due to the I^2t thermal rating limit of power supplies, the EFCCs coil current was programmed with a quick jump to 8 kAt within 200 ms followed by a slow ramp of I_{EFCC} up to 34 kAt with a duration of 3 s as shown in Fig. 4, to get a longer duration of the mitigated ELM phase at higher amplitude of I_{EFCC}. It seems that I_{EFCC} of 8 kAt is already above the threshold of ELM mitigation (the minimum value of I_{EFCC} to get an increase in the ELM frequency) in this plasma configuration. The ELM frequency, f_{ELM}, increased from ~ 20 Hz to ~ 70 Hz following the slow rise of I_{EFCC}. No locked mode was observed in this plasma even at the maximum I_{EFCC}, which is different to the locked mode threshold observed previously with a same value of q_{95} [9]. The increase in locked mode threshold can be attributed to the higher plasma density (30%) in this discharge caused by a change of strike points positions on the divertor plates [11]. The strike points of the previous discharges in reference [9] were located in the corners close to the divertor louvre yielding a high pumping efficiency.

To identify the character of the mitigated ELMs a heating power scan with four different levels of NBI power, P_{NBI}, of 10, 11.2, 14, 15.2 MW has been carried out. Fig. 5 shows the ELM frequency as a function of P_{NBI}. The frequency of the mitigated ELMs increases when P_{NBI} is increased. The power dependence of the ELM frequency is similar to normal type-I ELMs (as shown in the case without $n = 1$ field). However, the mitigated ELMs with $n = 1$ field have a higher frequency and are smaller in size.

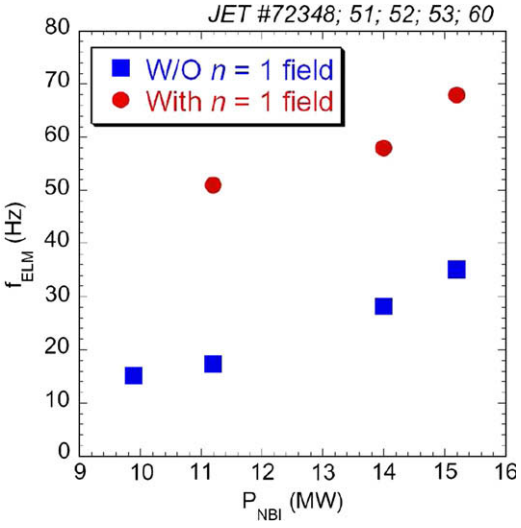

Fig. 5. Heating power dependence of ELM frequency measured during the phases with and without an $n = 1$ field.

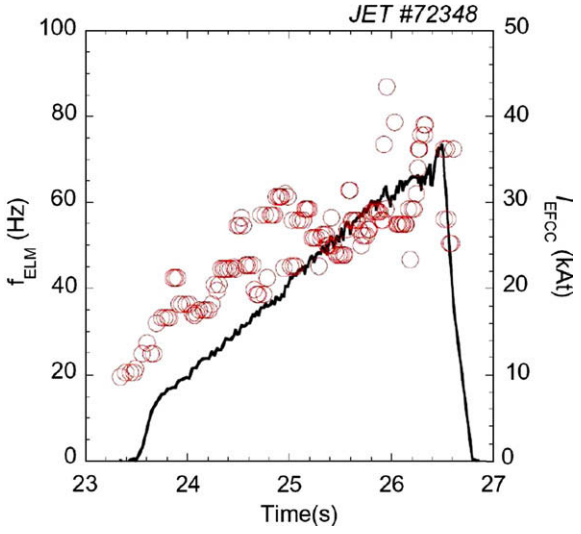

Fig. 4. Time evolution of ELM frequency, f_{ELM}, and EFCC coil current, I_{EFCC}.

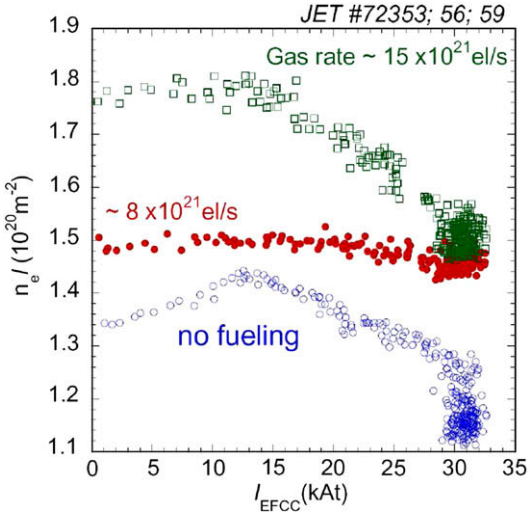

Fig. 6. Central line integrated density as a function of I_{EFCC} for the discharges with and without gas fueling.

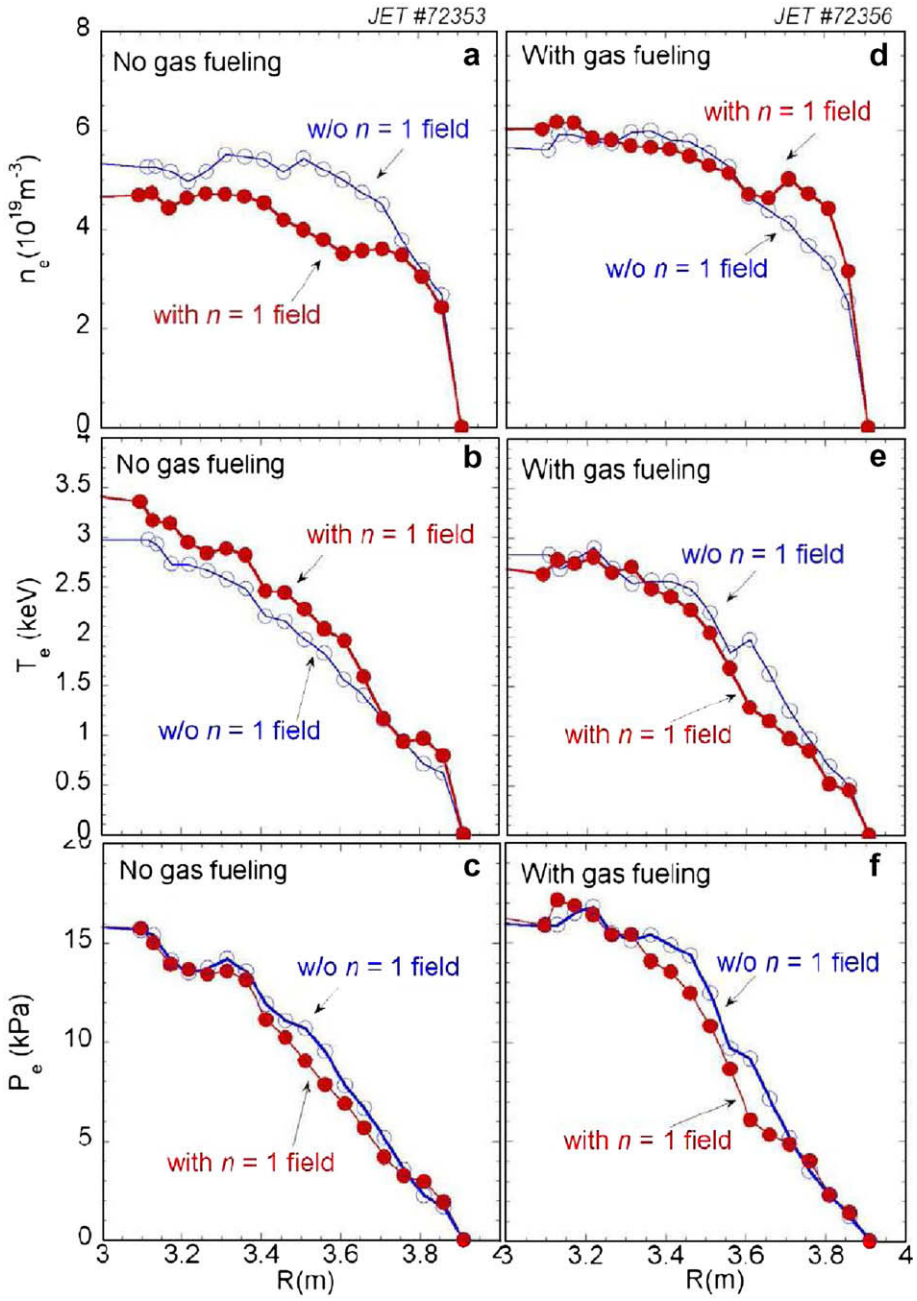

Fig. 7. The profiles of (a, d) electron density, n_e, (b, e) electron temperature, T_e, and (c, f) electron pressure, P_e, in discharges with and without gas fueling before and during the $n = 1$ EFCC application. The total gas rate is 7.8×10^{21} el/s for the fueled discharge.

5. Compensation of density pump-out with gas puffing

Compensation of the density pump-out effect due to the application of the external $n = 1$ field has been performed with gas puffing on JET. The target plasma in this experiment is chosen from the power scan in the ITER baseline scenario described in the previous section. The gas puffing started just after the injection of NBI and ~ 1 s before the $n = 1$ field was applied. The total gas puffing rate was systematically increased from discharge to discharge from 4.2, 7.8, 11.9, up to 15.4×10^{21} el/s keeping the same NBI input power of ~ 11.2 MW.

Fig. 6 shows that the central line integrated electron density as function of I_{EFCC}. Without additional gas fueling, the electron density starts to drop at $I_{EFCC} = 13$ kAt. The reduction of $n_e l$, $\Delta n_e l$, due to the pump-out effect does linearly depend on the amplitude of I_{EFCC}. However, a contiguous drop in $n_e l$ is observed even after I_{EFCC} reached the flat top value, which may indicate that full stationarity has not been reached in the unfuelled case. The Greenwald fraction, f_{GW}, drops from 0.68 to 0.55. When gas puffing is applied with a total gas rate of 7.8×10^{21} el/s, the target plasma density increased ($f_{GW} = 0.73$) and maintains a constant value even with application of the $n = 1$ perturbation field. The further increase of the gas fueling rate up to 15.4×10^{21} el/s yields a Greenwald density of $f_{GW} = 0.95$ before application of the $n = 1$ field, however, the plasma density drop with increasing I_{EFCC} appears again after the critical I_{EFCC} of 13 kAt was exceeded. These results demonstrate that there is an optimised fueling rate for the compensation of the density pump-out effect. Nevertheless, the plasma confinement becomes worse when the plasma density is chosen too high (close to Greenwald Limit) in the low triangularity target

plasma. There is a limitation to achieve a high plasma density without degradation of plasma confinement with an $n = 1$ field in low triangularity plasmas. Further investigation of the ELM mitigation with an $n = 1$ field will be performed in high density, high triangularity plasmas in the near future. However, it should be noted that there is no further drop of the density during the flat top of I_{EFCC} in the discharges with gas fueling.

Fig. 7(a)–(f) shows the influence of an $n = 1$ field on the profiles of n_e, T_e and P_e for the discharges with (a)–(c) no gas fueling and (d)–(f) optimised gas fueling at a rate of 7.8×10^{21} el/s. Without gas fueling, the application of an $n = 1$ field lets the density drop everywhere from core to edge while the electron temperature increases in the core stronger than that at the plasma edge. The electron collisionality at the pedestal dropped from 0.45 to 0.16. By application of gas fueling, both, plasma density and temperature in the plasma core remain the same as before. However, an increase of the edge density and a drop in the edge temperature are observed. The electron density profile is getting flatter with gas fueling, while the temperature profile becomes steeper in the plasma core. This results in an increase of the electron pedestal collisionality from 0.45 to 0.6. A similar influence of an $n = 1$ field on the electron pressure profile has been observed in plasmas with and without gas fueling as shown in Fig. 7(c) and (f). With an $n = 1$ field, the core electron pressure remains while the profile becomes slightly steeper due to a modest reduction of the electron pressure at plasma edge. The measurement of the diamagnetic loop shows that there was about ~10% drop in plasma stored energy when the $n = 1$ field was applied. No difference in the stored energy between the discharges with and without an optimised gas fueling has been found. However, a further increase in the gas puffing rate above the optimised value will result in a large reduction of the plasma stored energy up to 20–25%. The electron pedestal collisionality is increased up to 2.0. It should be noted that there is no detachment and no MARFE is observed in the target plasmas even with a fueling rate up to 15.4×10^{21} el/s.

The influence of gas fueling on the frequency of ELMs is plotted in Fig. 8 for both cases, with and without application of the $n = 1$ field. Below the optimised fueling rate, the mitigated ELM frequency stays almost at a similar frequency of 50–60 Hz, while the target plasma has an ELM frequency of 20–25 Hz. Once the gas rate increases over the optimised value, a rise of the ELM frequencies is observed in both cases.

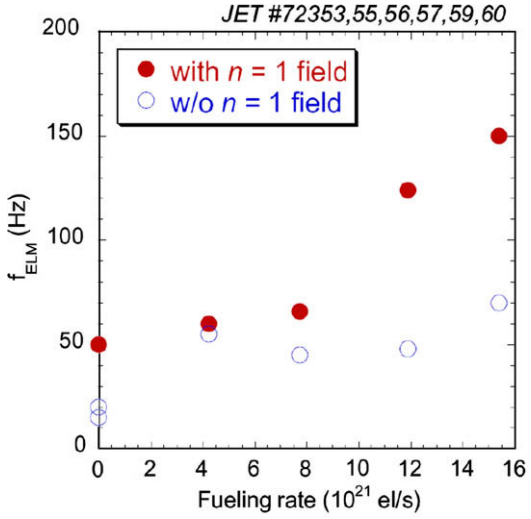

Fig. 8. ELM frequency as a function of the total gas fueling rate measured with and without an $n = 1$ field.

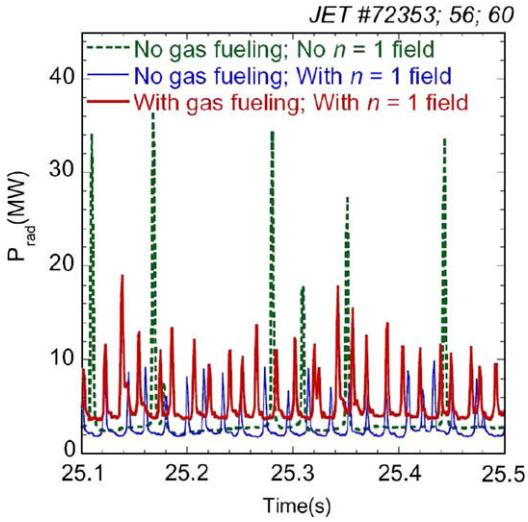

Fig. 9. Time trace of total radiation, P_{rad}, during application of an $n = 1$ field for discharges with and without fueling. The total gas rate is 7.8×10^{21} el/s for the fueled discharge.

Fig. 9 shows a comparison of the total radiation between the discharges with and with out an $n = 1$ field, and with and without a gas fueling during the ELM mitigation phase. For the discharge with no gas fueling, no clear change in the total radiated power measured in the inter-ELM phase caused by the application of the $n = 1$ field could be detected, even when the ELM frequency increased by a factor of ~4. However, the ELM peak radiation dropped significantly for the mitigated ELMs, which is mainly due to a reduction of carbon erosion when the ELMs become smaller in size. With an optimised gas puffing, the total radiated power measured in the inter-ELM phase increased by a factor of 2, which is about ~30% of the total heating power while the decrease of the ELM peak radiation is not that pronounced.

6. Summary and conclusion

Active ELM control by using static external magnetic perturbation fields with low n, has been demonstrated for both, ITER baseline ($q_{95} \sim 3$) and high beta advanced tokamak steady state scenarios at the JET tokamak. ELM control was found to work in high beta plasmas (β_N up to 2.9) without degradation of the energy confinement time. These results confirm that the ELM mitigation using an low n perturbation has a wide operational window for different target plasmas. An increase of the frequency of mitigated ELMs with increasing NBI heating power has been observed, which shows that mitigated ELM with $n = 1$ field have a similar power scaling as type-I ELMs. The ELM mitigation with the $n = 1$ field has been performed in low triangularity plasmas with additional gas fueling. The plasma density can be maintained during the flat top of I_{EFCC}, while a contiguous drop in density even at a constant I_{EFCC} in discharges without gas fueling has been observed.

In conclusion, the experimental results from JET show that both the frequency and the amplitude of type-I ELMs can be actively controlled with an acceptable reduction in plasma confinement by the application of an $n = 1$ perturbation field generated by external coils. During the application of the low n field the ELM frequency increased by a factor of ~4–5. Reduction in carbon erosion and ELM peak heat fluxes on the divertor target by roughly the same factor as the increase of the ELM frequency has been observed. Compensation of the density pump-out effect has been achieved by means of gas fueling in low triangularity plasmas.

An optimised fueling rate to compensate the density pump-out effect has been identified.

Acknowledgements

This work, supported by the European Communities under the contract of Association between EURATOM and FZJ, was carried out within the framework of the European Fusion Development Agreement. The views and opinions expressed herein do not necessarily reflect those of the European Commission.

References

[1] ITER physics basis, Nucl. Fusion 39 (1999) 2137.
[2] F. Wagner et al., Phys. Rev. Lett. 49 (1982) 1408.
[3] J.W. Connor, Plasma Phys. Control. Fus. 40 (1998) 531.
[4] A. Loarte et al., J. Nucl. Mater. 313–316 (2003) 962.
[5] T. Evans et al., Nature Phys. 2 (2006) 419.
[6] T. Evans et al., Phys. Rev. Lett. 92 (2004) 235003.
[7] I. Barlow et al., Fus. Eng. Des. 58&59 (2001) 189.
[8] Y. Liang et al., Phys. Rev. Lett. 98 (2007) 265004.
[9] Y. Liang et al., Plasma Phys. Control. Fus. 49 (2007) B581.
[10] J.C. Vallet et al., Phys. Rev. Lett. 67 (1991) 2662.
[11] E. Lazzaro et al., Phys. Plasmas 9 (2002) 3906.
[12] R.V. Budny et al., Nucl. Fus. 35 (1995) 1497.
[13] X. Litaudon et al., Plasma Phys. Control. Fus. 49 (2007) B529B550.
[14] H.R. Koslowski et al., in: Proceedings of the 34th EPS Conference on Plasma Physics Warsaw, 2–6 July 2007 ECA, vol. 31F, 2007, P-5.135.
[15] R.J. Buttery et al., Nucl. Fus. 39 (1999) 1827.
[16] H.R. Koslowski et al., Nucl. Fus. 46 (2006) L1.
[17] S. Jachmich et al., in: Proceedings of the 34th EPS Conference on Plasma Physics, Warsaw, 2–6 July 2007 ECA vol. 31F, 2007, P-5.099.
[18] H.G. Esser et al., J. Nucl. Mater. 337–339 (2005) 84.